Simulation of Voltage and Current Distributions in Transmission Lines Using State Variables and Exponential Approximation

Panuwat Dan-Klang and Ekachai Leelarasmee

A new method for simulating voltage and current distributions in transmission lines is described. It gives the time domain solution of the terminal voltage and current as well as their line distributions. This is achieved by treating voltage and current distributions as distributed state variables (DSVs) and turning the transmission line equation into an ordinary differential equation. Thus the transmission line is treated like other lumped dynamic components, such as capacitors. Using backward differentiation formulae for time discretization, the DSV transmission line component is converted to a simple time domain companion model, from which its local truncation error can be derived. As the voltage and current distributions get more complicated with time, a new piecewise exponential with controllable accuracy is invented. A segmentation algorithm is also devised so that the line is dynamically bisected to guarantee that the total piecewise exponential error is a small fraction of the local truncation error. Using this approach, the user can see the line voltage and current at any point and time freely without explicitly segmenting the line before starting the simulation.

Keywords: Exponential approximation, piecewise interpolation distributed state variable, transmission line.

Manuscript received Sept. 12, 2008; revised Dec. 17, 2008; accepted Dec. 24, 2008.

This work was supported by the Thailand Research Fund and Chulalongkorn University Ratchadapiseksompoj Fund, Thailand.

Panuwat Dan-Klang (phone: +662 218 6488, email: eepanuwatdk@gmail.com) and Ekachai Leelarasmee (email: ekachai.l@chula.ac.th) are with the Electrical Engineering Department, Chulalongkorn University, Patumwan, Bangkok, Thailand.

I. Introduction

A transmission line, as shown in Fig. 1, is an important component found in both power and communication distribution networks. It also appears in electrical circuits in various forms such as microstrips, coaxial cables, and high-speed interconnects in integrated circuits. At low frequency, the line can be treated as being short circuited or replaced by lumped components. However, for high-frequency applications, such as high-voltage spike and high-speed communication, the line can have a significant effect on the dynamic of the circuit with which the line is connected. Hence, a transient simulation that treats a transmission line as a dynamic component must be developed. The dynamic equation is usually described by the telegraph equation [1], which consists of a set of linear partial differential equations comprising both temporal and spatial derivatives of line voltages and currents:

$$\begin{aligned} \frac{\partial v(x,t)}{\partial x} &= -L\frac{\partial i(x,t)}{\partial t} - Rv(x,t), \\ \frac{\partial i(x,t)}{\partial x} &= -C\frac{\partial v(x,t)}{\partial t} - Gi(x,t). \end{aligned} \tag{1}$$

Such a formulation significantly differs from lumped components, that is, capacitor and inductor, which are described only by differential equations, such as $i = C(dv/dt)$ or $v = L(di/dt)$. Hence, the telegraph equation does not fit with the equation formulation procedure of conventional circuit simulators, such as Hspice [2], EMTP [3], and MultiSim [4]. Moreover, its frequency domain terminal characteristic is an irrational function of the complex frequency s. Thus, the line

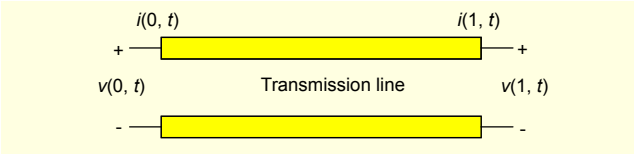

Fig. 1. Transmission line model.

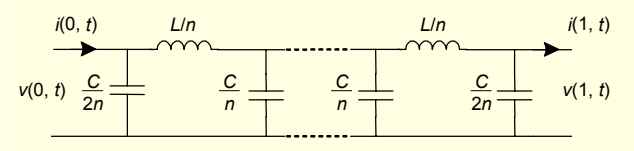

Fig. 2. Transmission line modeled as n segments of lumped components.

terminals cannot be accurately modeled by a finite number of lumped components. An exact calculation of its transient response is impossible except for some special cases, such as R=0 and G=0 [1].

During the past three decades, various methods have been developed to approximate the dynamic of the transmission line to allow the transient solution of the transmission line circuit to be numerically computable. The methods can be classified according to the selected domain of approximation, namely, frequency or spatial approximation.

The frequency approximation methods focus on approximating the terminal frequency responses of a transmission line with rational functions that has a finite number of poles. They are usually referred to as model order reduction (MOR) [5] methods. The simplest method of this class is the segmentation method, which replaces a transmission line with a large number (e.g. 100) of segments of lumped R, L, G, and C components as shown in Fig. 2. More efficient and accurate MOR methods have been proposed, such as PRIMA [6], [7] and DOMMEL [8], [9].

Frequency approximation methods have been shown to reduce the complexity of computing the time domain companion model of a transmission line. However, once the approximation is carried out, the original telegraph equation is no longer used in the transient analysis. That is, the reduced model is determined *a priori*. Hence, even if the time discretization, that is, the backward differentiation formula [10], is carried out using very small time steps, the transient solution of a transmission line circuit will converge only to that of the reduced frequency model, not the original one. Furthermore, there is no explicit formula for determining the time domain error or accuracy of the frequency methods. Therefore, time accuracy control is not possible. Another disadvantage of the frequency approximation method is that only the transient results at the terminal ends of the line are calculated. If the user needs to find the transient at some internal points within the line, he/she has to divide the line at those points into several segments before starting the simulation.

The spatial approximation methods derive the time domain companion model directly from the telegraph equation. Two examples are the state-based [11] and the semi-discretization [12] methods. This companion model was shown to depend on the voltage and current distributions along the line at previous time points. Since the telegraph equation is used within the time iteration loop, the transient solution can converge to the exact solution as the time step is reduced. Unfortunately, the exact line voltage and current distributions cannot be analytically described; therefore, they must be approximated in the spatial domain by simple functions. Both the state-based and semi-discretization methods propose piecewise linear approximation. Moreover, they do not provide concrete details of the mechanism for controlling the accuracy of the piecewise linear approximation. Therefore, it is not clear whether its transient solution can be theoretically guaranteed to converge to the exact solution as the time step is reduced to increase transient accuracy.

This paper describes a variation of the distributed state variable (DSV) method for handling a transmission line in the time domain. The method was first introduced in [13]. It is a spatial approximation method, but it differs significantly from other previously mentioned methods in its derivation and implementation procedures. In the DSV method, line voltage and current distributions are treated as the state variables of the transmission line and are called DSVs. The telegraph equation can be transformed into a first-order state equation in terms of these DSVs. Thus, conventional backward differentiation techniques can be directly applied in the same way as other lumped dynamic components, such as capacitors and inductors. The method also gives the time domain companion model of a transmission line along with the formula to compute its local truncation error (LTE). This LTE is used to determine the appropriate time step. However, it will be shown that the DSVs become more complicated with time and more computationally expensive to track. To simplify these distributions, the piecewise exponential (PWE) function is proposed to be used where appropriate. However, the accuracy of this spatial approximation method is controlled by the computed LTE. The transient solution of the transmission line circuit can converge to the exact solution as the time step decreases because the LTE will also decrease. One advantage is that the line voltage and current distributions at all times are calculated and can be stored. Thus, users can view these distributions at any time or point without having to divide the line and restart the simulation.

This paper is organized as follows. The basic concept of the DSV method is given in section II. In section III, the PWE

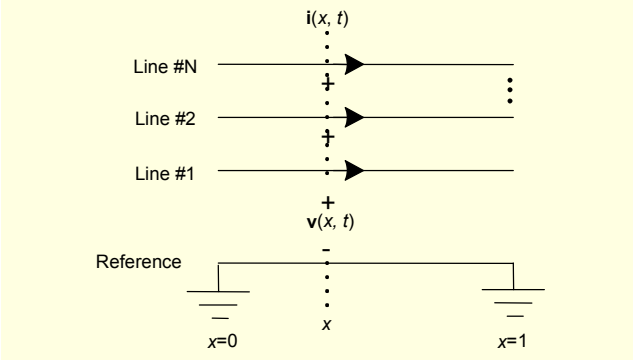

Fig. 3. N+1 coupled transmission line with the bottom line treated as a reference.

approximation is introduced to simplify these distributions at each time point and its error formula is derived. An algorithm which dynamically divides the transmission line into several segments is also described. A rigorous criterion for controlling the approximation errors that depend on the LTE is also suggested. Several examples are given in section IV to demonstrate how the method works.

II. Distributed State Variable

The type of transmission line considered in this paper is a set of N+1 coupled uniform transmission lines with the unit length as shown in Fig. 3.

Let the bottom line be treated as a reference line. The dynamic behavior of the other lines with respect to the reference line can be described by the telegraph equation as

$$\frac{\partial}{\partial x}\begin{bmatrix}\mathbf{v}(x,t)\\ \mathbf{i}(x,t)\end{bmatrix}=-\begin{bmatrix}0 & \mathbf{L}\\ \mathbf{C} & 0\end{bmatrix}\frac{\partial}{\partial t}\begin{bmatrix}\mathbf{v}(x,t)\\ \mathbf{i}(x,t)\end{bmatrix}-\begin{bmatrix}0 & \mathbf{R}\\ \mathbf{G} & 0\end{bmatrix}\begin{bmatrix}\mathbf{v}(x,t)\\ \mathbf{i}(x,t)\end{bmatrix}, \quad (2)$$

where $\mathbf{v}(x,t)$ and $\mathbf{i}(x,t)$ are vectors of N voltage and current distributions at distance x and time t with respect to the reference line; **L**, **C**, **R,** and **G** are $N\times N$ matrices of inductance, capacitance, resistance, and conductance measured as per unit distance and with respect to the reference line. To implement our analysis approach, the telegraph equation (2) can be formulated as

$$\frac{\partial}{\partial t}\begin{bmatrix}\mathbf{v}(x,t)\\ \mathbf{i}(x,t)\end{bmatrix}=-\mathbf{A}^{-1}\left(\mathbf{B}+\mathbf{I}\frac{\partial}{\partial x}\right)\begin{bmatrix}\mathbf{v}(x,t)\\ \mathbf{i}(x,t)\end{bmatrix}, \quad (3)$$

where $\mathbf{A}=\begin{bmatrix}0 & \mathbf{L}\\ \mathbf{C} & 0\end{bmatrix}$ and $\mathbf{B}=\begin{bmatrix}0 & \mathbf{R}\\ \mathbf{G} & 0\end{bmatrix}$.

If we simply treat $\partial/\partial x$ as an operator, then (3) can be viewed as an ordinary differential equation or state equation with $\begin{bmatrix}\mathbf{v}(x,t)\\ \mathbf{i}(x,t)\end{bmatrix}$ as its state. Therefore, we call $\begin{bmatrix}\mathbf{v}(x,t)\\ \mathbf{i}(x,t)\end{bmatrix}$ the DSV of the transmission line, and we call (3) the DSV formulation of the telegraph equation. This formulation allows us to treat the whole set of coupled transmission lines as a single dynamic component in the same way as we treat a capacitor or an inductor because they are all described by state equations. Therefore, all numerical steps used to deal with capacitors and inductors in the transient simulation can be applied directly to the transmission line. That is, the time derivative of its state variable must first be discretized by the well known backward differentiation formula [11]. In this paper, we shall apply the backward Euler differentiation formula with time step $h_n=t_n-t_{n-1}$ to approximate the time derivative in (3) at time t_n as

$$\frac{1}{h_n}\left[\begin{bmatrix}\mathbf{v}_n(x)\\ \mathbf{i}_n(x)\end{bmatrix}-\begin{bmatrix}\mathbf{v}_{n-1}(x)\\ \mathbf{i}_{n-1}(x)\end{bmatrix}\right]=-\mathbf{A}^{-1}\left(\mathbf{B}+\mathbf{I}\frac{\partial}{\partial x}\right)\begin{bmatrix}\mathbf{v}_n(x)\\ \mathbf{i}_n(x)\end{bmatrix}, \quad (4)$$

where $\begin{bmatrix}\mathbf{v}_n(x)\\ \mathbf{i}_n(x)\end{bmatrix}$ is the approximated solution of $\begin{bmatrix}\mathbf{v}(x,t_n)\\ \mathbf{i}(x,t_n)\end{bmatrix}$, and $\begin{bmatrix}\mathbf{v}(x,0)\\ \mathbf{i}(x,0)\end{bmatrix}$ is the vector of the initial line voltage and current distributions. Without loss of generality, we assume that $\begin{bmatrix}\mathbf{v}(x,0)\\ \mathbf{i}(x,0)\end{bmatrix}=0$ for all $x\in[0,1]$. Note that (4) is a recursive equation describing the distribution at t_n in terms of its previous value at t_{n-1}. After some algebraic manipulation, this equation can be rewritten as

$$\frac{d}{dx}\begin{bmatrix}\mathbf{v}_n(x)\\ \mathbf{i}_n(x)\end{bmatrix}=\mathbf{M}_n\begin{bmatrix}\mathbf{v}_n(x)\\ \mathbf{i}_n(x)\end{bmatrix}+\mathbf{D}_n\begin{bmatrix}\mathbf{v}_{n-1}(x)\\ \mathbf{i}_{n-1}(x)\end{bmatrix}, \quad (5)$$

where $\mathbf{M}_n=-\left[\frac{\mathbf{A}}{h_n}+\mathbf{B}\right]$ and $\mathbf{D}_n=\frac{\mathbf{A}}{h_n}$.

The recursive property of (5) can be combined from 0 to t_n in the following matrix form:

$$\frac{dy(x)}{dx}=\Gamma y(x), \quad (6)$$

where

$$\mathbf{y}(x)=\begin{bmatrix}\mathbf{v}_1(x)\\ \mathbf{i}_1(x)\\ \mathbf{v}_2(x)\\ \mathbf{i}_2(x)\\ \vdots\\ \mathbf{v}_n(x)\\ \mathbf{i}_n(x)\end{bmatrix} \text{ and } \Gamma=\begin{bmatrix}\mathbf{M}_1 & 0 & 0 & 0\\ \mathbf{D}_2 & \mathbf{M}_2 & 0 & 0\\ 0 & \ddots & \ddots & \vdots\\ 0 & 0 & \mathbf{D}_n & \mathbf{M}_n\end{bmatrix}. \quad (7)$$

From this, the solution of (6) can be solved to obtain

$$\begin{bmatrix}\mathbf{v}_n(x)\\ \mathbf{i}_n(x)\end{bmatrix} = [0,\cdots,\mathbf{I}]e^{\Gamma x}y(0)$$
$$= \left[\psi_1(x),\ \cdots,\ \psi_{n-1}(x),\ e^{\mathbf{M}_n x}\right]y(0)\,. \quad (8)$$

This equation can be rewritten as

$$\begin{bmatrix}\mathbf{v}_n(x)\\ \mathbf{i}_n(x)\end{bmatrix} = \exp(\mathbf{M}_n x)\begin{bmatrix}\mathbf{v}_n(0)\\ \mathbf{i}_n(0)\end{bmatrix} + \Psi_n(x)\,,\ \ x\in[0,1], \quad (9)$$

where

$$\Psi_n(x) = \sum_{i=1}^{n-1}\psi_i(x)\begin{bmatrix}\mathbf{v}_i(0)\\ \mathbf{i}_i(0)\end{bmatrix}. \quad (10)$$

With $x=1$, we obtain the following relationship between the line terminal voltages and currents:

$$\begin{bmatrix}\mathbf{v}_n(1)\\ \mathbf{i}_n(1)\end{bmatrix} = \exp(\mathbf{M}_n)\begin{bmatrix}\mathbf{v}_n(0)\\ \mathbf{i}_n(0)\end{bmatrix} + \Psi_n(1)\,. \quad (11)$$

This equation describes the time domain companion model of the transmission line with respect to its terminals on both ends, where $\Psi_n(1)$ is a constant term whose calculating formula is described in the appendix. To comply with the nodal equation formulation, we perform some matrix operations and obtain the following input admittance matrix of the transmission line as well as its model given in Fig. 4:

$$\begin{bmatrix}\mathbf{i}_n(0)\\ \mathbf{i}_n(1)\end{bmatrix} = \mathbf{Z}_n^{-1}\begin{bmatrix}(\tanh(\Lambda_n))^{-1} - (\sinh(\Lambda_n))^{-1}\\ (\sinh(\Lambda_n))^{-1} - (\tanh(\Lambda_n))^{-1}\end{bmatrix}\begin{bmatrix}\mathbf{v}_n(0)\\ \mathbf{v}_n(1)\end{bmatrix} + \begin{bmatrix}\mathbf{J}_0\\ \mathbf{J}_1\end{bmatrix}, \quad (12)$$

where $\mathbf{Z}_n$ and Λ_n are such that

$$\mathbf{A}_n = \begin{bmatrix}\mathbf{I} & \mathbf{Z}_n\\ \mathbf{I} & -\mathbf{Z}_n\end{bmatrix}^{-1}\begin{bmatrix}-\Lambda_n & 0\\ 0 & \Lambda_n\end{bmatrix}\begin{bmatrix}\mathbf{I} & \mathbf{Z}_n\\ \mathbf{I} & -\mathbf{Z}_n\end{bmatrix},$$

$$\begin{bmatrix}\mathbf{J}_0\\ \mathbf{J}_1\end{bmatrix} = \mathbf{Z}_n^{-1}(\exp(\Lambda_n) - \exp(-\Lambda_n))^{-1}\begin{bmatrix}\mathbf{I} & \mathbf{I}\\ \exp(\Lambda_n) & \exp(-\Lambda_n)\end{bmatrix}\Psi_n(1),$$

where $\mathbf{Y}_{12} = \mathbf{Z}_n^{-1}\sinh^{-1}(\Lambda_n)$ and $\mathbf{Y}_1 = \mathbf{Y}_2 = \mathbf{Z}_n^{-1}\tanh^{-1}(\Lambda_n)$.

A standard circuit simulator can then use this companion model along with the companion models of other components, such as capacitors and inductors to set up the circuit matrix equation at time t_n. Once, the circuit equation is solved, $\mathbf{v}_n(0)$, $\mathbf{i}_n(0)$, $\mathbf{v}_n(1)$, and $\mathbf{i}_n(1)$ can be used to determine the distribution $\begin{bmatrix}\mathbf{v}_n(x)\\ \mathbf{i}_n(x)\end{bmatrix}$ according to the differential equation in (4). The DSV approach also allows the calculation of the LTE of the line as

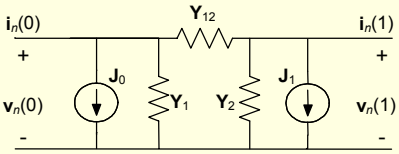

Fig. 4. Companion model of transmission line at both ends.

$$LTE_n = \left\| \begin{bmatrix}\mathbf{v}_n(x)\\ \mathbf{i}_n(x)\end{bmatrix} - \begin{bmatrix}\tilde{\mathbf{v}}_n(x)\\ \tilde{\mathbf{i}}_n(x)\end{bmatrix} \right\|, \quad (13)$$

where $\begin{bmatrix}\tilde{\mathbf{v}}_n(x)\\ \tilde{\mathbf{i}}_n(x)\end{bmatrix}$ is the predicted value of $\begin{bmatrix}\mathbf{v}_n(x)\\ \mathbf{i}_n(x)\end{bmatrix}$. Here, the norm is defined by

$$\|\mathbf{y}(\cdot)\|^2 \equiv \int_0^1 \mathbf{y}^T(x)\mathbf{T}^T\mathbf{T}\mathbf{y}(x)\,dx\,, \quad (14)$$

where $\mathbf{T}$ is a $2N\times 2N$ non-singular matrix used to weigh the voltage and current distributions. Since the first-order backward differentiation formula is used in the time discretization, the predicted value should be the first-order forward differentiation formula [8], that is,

$$\begin{bmatrix}\tilde{\mathbf{v}}_n(x)\\ \tilde{\mathbf{i}}_n(x)\end{bmatrix} = \begin{bmatrix}\mathbf{v}_{n-1}(x)\\ \mathbf{i}_{n-1}(x)\end{bmatrix} + \frac{h_n}{h_{n-1}}\left\{\begin{bmatrix}\mathbf{v}_{n-1}(x)\\ \mathbf{i}_{n-1}(x)\end{bmatrix} - \begin{bmatrix}\mathbf{v}_{n-2}(x)\\ \mathbf{i}_{n-2}(x)\end{bmatrix}\right\}. \quad (15)$$

The actual procedure for computing LTE_n is given in the appendix. The computed LTE of the line is then used to determine the next time step, $h_{n+1}=t_{n+1}-t_n$, along with the LTE of the other lumped dynamic components.

III. Piecewise Exponential Approximation

To study the computation complexity of the DSV method, we note that $\mathbf{M}_n$ is a $2N\times 2N$ matrix. It follows that $\begin{bmatrix}\mathbf{v}_n(x)\\ \mathbf{i}_n(x)\end{bmatrix}$ has $2Nn$ exponential terms. Thus, the total computational complexity of the DSV at time t_n is of the order $\sum_1^n 2Ni = Nn(n+1)$. Moreover, the DSV method that we described in (8) must store all past values of voltage and current at $x=0$, that is, $\begin{bmatrix}\mathbf{v}_i(0)\\ \mathbf{i}_i(0)\end{bmatrix}; i=1,\cdots,N-1$ in order to obtain $\begin{bmatrix}\mathbf{v}_n(x)\\ \mathbf{i}_n(x)\end{bmatrix}$ according to (9). This fast growing rate of computation and storage requirement is a serious drawback. To alleviate this problem at t_{n+1}, we propose to approximate $\begin{bmatrix}\mathbf{v}_n(x)\\ \mathbf{i}_n(x)\end{bmatrix}$ with a simplified function $\begin{bmatrix}\hat{\mathbf{v}}_n(x)\\ \hat{\mathbf{i}}_n(x)\end{bmatrix}$ of the following form:

$$\begin{bmatrix}\hat{\mathbf{v}}_n(x)\\ \hat{\mathbf{i}}_n(x)\end{bmatrix} = \exp(\hat{\mathbf{M}}x)\begin{bmatrix}\mathbf{v}_n(x)\\ \mathbf{i}_n(x)\end{bmatrix} \approx \begin{bmatrix}\mathbf{v}_n(x)\\ \mathbf{i}_n(x)\end{bmatrix}. \quad (16)$$

Once $\hat{\mathbf{M}}$ is obtained, the calculation of $\mathbf{w}_{n+1}(x)$ becomes

$$\frac{d}{dx}\begin{bmatrix}\hat{\mathbf{v}}_n(x)\\ \hat{\mathbf{i}}_n(x)\\ \mathbf{v}_{n+1}(x)\\ \mathbf{i}_{n+1}(x)\end{bmatrix} = \begin{bmatrix}\hat{\mathbf{M}} & 0\\ \mathbf{D}_{n+1} & \mathbf{M}_{n+1}\end{bmatrix}\begin{bmatrix}\hat{\mathbf{v}}_n(x)\\ \hat{\mathbf{i}}_n(x)\\ \mathbf{v}_{n+1}(x)\\ \mathbf{i}_{n+1}(x)\end{bmatrix}, \quad (17)$$

which is much simpler than using (7) or (8).

A good strategy for finding $\hat{\mathbf{M}}$ would be to let $\begin{bmatrix}\hat{\mathbf{v}}_n(x)\\ \hat{\mathbf{i}}_n(x)\end{bmatrix}$ interpolate $\begin{bmatrix}\mathbf{v}_n(x)\\ \mathbf{i}_n(x)\end{bmatrix}$ as much as possible. Therefore, we choose $2N$+1 interpolating points evenly distributed within the segment, that is,

$$x_i = \frac{i}{2N}, \qquad i = 0,1,\cdots,2N.$$

Substituting x_i in (16), we have

$$\exp(\hat{\mathbf{M}}i/2N)\begin{bmatrix}\mathbf{v}_n(0)\\ \mathbf{i}_n(0)\end{bmatrix} = \begin{bmatrix}\mathbf{v}_n(\frac{i}{2N})\\ \mathbf{i}_n(\frac{i}{2N})\end{bmatrix}, \quad i = 1,\cdots,2N. \quad (18)$$

Because it is an exponential function, it can be deduced that

$$\exp(\hat{\mathbf{M}}i/2N)\begin{bmatrix}\mathbf{v}_n(\frac{i-1}{2N})\\ \mathbf{i}_n(\frac{i-1}{2N})\end{bmatrix} = \begin{bmatrix}\mathbf{v}_n(\frac{i}{2N})\\ \mathbf{i}_n(\frac{i}{2N})\end{bmatrix}, \quad i = 1,\cdots,2N. \quad (19)$$

In matrix form, this becomes

$$\exp(\hat{\mathbf{M}}/2N)\mathbf{W}_0 = \mathbf{W}_1, \quad (20)$$

where

$$\mathbf{W}_0 = \begin{bmatrix}\mathbf{v}_n(0), & \mathbf{v}_n(\frac{1}{2N}), & \ldots., & \mathbf{v}_n(\frac{2N-1}{2N})\\ \mathbf{i}_n(0), & \mathbf{i}_n(\frac{1}{2N}), & \ldots., & \mathbf{i}_n(\frac{2N-1}{2N})\end{bmatrix},$$

and

$$\mathbf{W}_1 = \begin{bmatrix}\mathbf{v}_n(\frac{1}{2N}), & \mathbf{v}_n(\frac{2}{2N}), & \ldots., & \mathbf{v}_n(\frac{2N}{2N})\\ \mathbf{i}_n(\frac{1}{2N}), & \mathbf{i}_n(\frac{2}{2N}), & \ldots., & \mathbf{i}_n(\frac{2N}{2N})\end{bmatrix}.$$

Thus,

$$\hat{\mathbf{M}} = 2N\ln(\mathbf{W}_1\mathbf{W}_0^{-1})`. \quad (21).$$

To maintain accuracy with respect to the transient simulation, the approximating function is accepted only when $\begin{bmatrix}\hat{\mathbf{v}}_n(x)\\ \hat{\mathbf{i}}_n(x)\end{bmatrix}$ is close to $\begin{bmatrix}\mathbf{v}_n(x)\\ \mathbf{i}_n(x)\end{bmatrix}$ within a small percentage of its local truncation error. Therefore, the criteria for accepting the approximation is

$$ERR = \left\| \begin{bmatrix}\hat{\mathbf{v}}_n(x)\\ \hat{\mathbf{i}}_n(x)\end{bmatrix} - \begin{bmatrix}\mathbf{v}_n(x)\\ \mathbf{i}_n(x)\end{bmatrix} \right\| < \alpha LTE_n, \text{ where } \alpha << 1.$$

Otherwise, the approximation is not successful, and the segment is divided into two halves using a bisection algorithm, each of which is approximated by its own exponential function using the techniques described above. This time, the errors of the two segments are added before they are tested. If they still fail the test, only the segment that has the largest error will be divided. At the same time two adjacent segments may be combined if their error is acceptable. Hence, we are now ready to suggest the following segmentation algorithm.

Step 1. Set K=1 and $\alpha << 1$. That is, treat the whole line as one segment.

Step 2. Compute $\hat{\mathbf{M}}_i$ and ERR_i, $i = 1,\cdots,K$.

Step 3. Calculate $ERR = \sqrt{\sum_{i=1}^{K} ERR_i^2}$.

Step 4. If $ERR \le \alpha \cdot LTE_n$, exit.

Step 5. Determine $\hat{i}$ such that

$$ERR_{\hat{i}} = \max(ERR_i, i = 1,\cdots,K).$$

Step 6. Divide the $\hat{i}$-th segment into two at its middle point.

Step 7. Set K=K+1 and go to step 2.

IV. Numerical Examples

The DSV with the piecewise exponential approximation (PEA) methods has been tested with 5 transmission line circuits using MATLAB to verify the calculations. Where applicable, all results are compared with a standard circuit simulator, Hspice [2]. The first circuit, shown in Fig. 5, consists of 4 uncoupled lossy transmission lines. The parameters of each transmission line are L=1 mH/m, C =1 μF/m, G =0 S/m, and R = 1 Ω/m. Each line is one meter long and starts with zero voltage and current distributions. Its unit step input has a 0.1 ms rise time. This circuit is simulated using 0.5 mV local truncation error, and the approximation error factor is α = 0.1. The simulated waveform at the load-end of line 1 is shown in Fig. 6. It is indistinguishable from the results of Hspice [2]. Figure 7 shows how the lines are segmented dynamically, and the maximum number of segments is 15. However, this number gradually decreases to 1 segment when the line

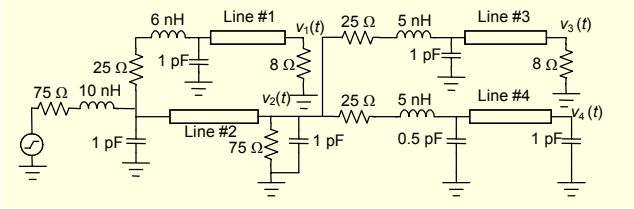

Fig. 5. Circuit diagram of 4 uncoupled lossy transmission lines (0.1 ms).

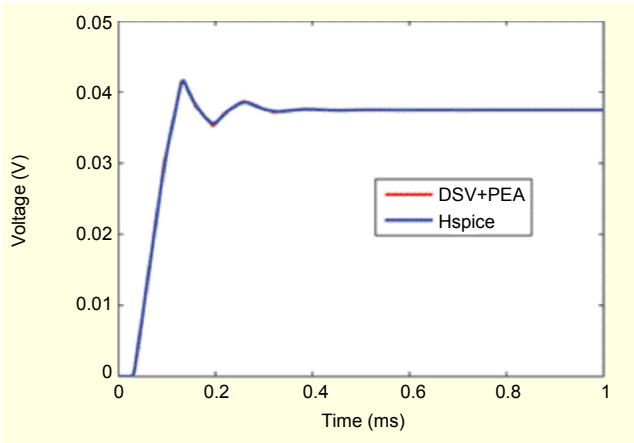

Fig. 6. Voltage waveform at the $v_1(t)$ of the circuit in Fig. 5. Allowable local truncation error is 0.5 mV, and approximation error factor α is 0.1.

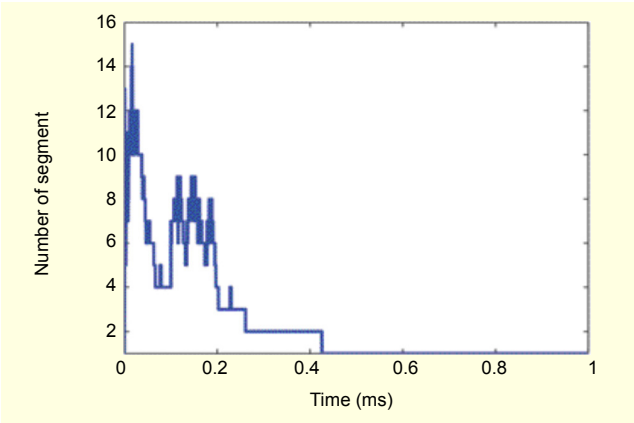

Fig. 7. Variation of number of exponential segments with time of line 1 of the circuit shown in Fig. 5 at various time points.

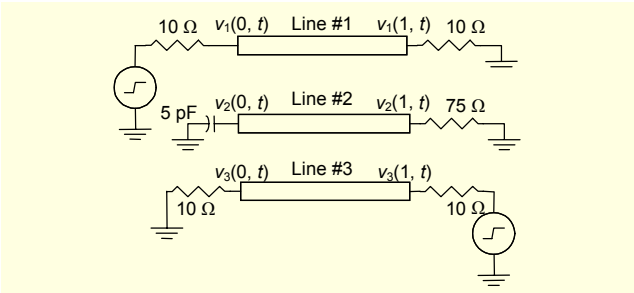

Fig. 8. Circuit comprising 3 lossy transmission lines.

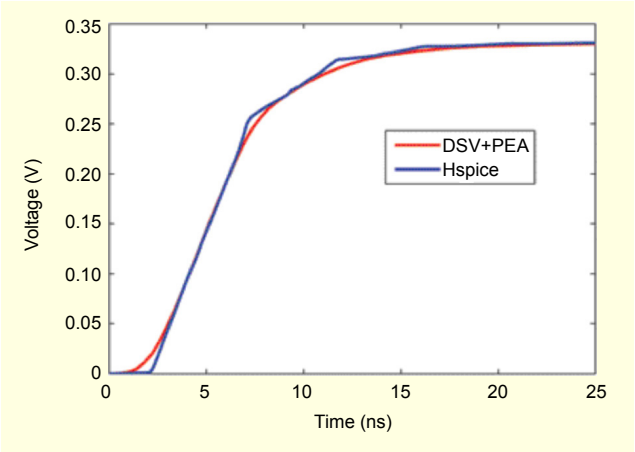

Fig. 9. Simulated waveform at the right end of the top line of the circuit in Fig. 8. Allowable local truncation error is 0.5 mV, and approximation error α is 0.1.

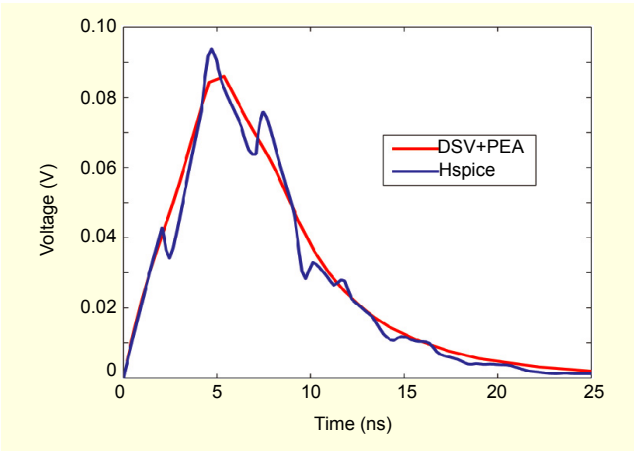

Fig. 10. Voltage waveform at $v_2(1, t)$ of the circuit shown in Fig. 8.

activities reach the DC steady state; therefore, the execution time can be fast.

The circuit in the second example, shown in Fig. 8, consists of three joined transmission lines (N=3). The lines are 1 meter long with the following parameters:

$$\mathbf{R}=\begin{bmatrix}10 & 0 & 0\\ 0 & 10 & 0\\ 0 & 0 & 10\end{bmatrix}\Omega/\text{m},\quad \mathbf{G}=\begin{bmatrix}1 & 0 & 0\\ 0 & 1 & 0\\ 0 & 0 & 1\end{bmatrix}\text{mS/m},$$

$$\mathbf{L}=\begin{bmatrix}100 & 25 & 2.5\\ 25 & 100 & 25\\ 2.5 & 25 & 100\end{bmatrix}\text{nH/m},\quad \mathbf{C}=\begin{bmatrix}50 & -10 & -1\\ -10 & 60 & -10\\ -1 & -10 & 50\end{bmatrix}\text{pF/m}.$$

The circuit has two unit step inputs, one at the top line and the other at the bottom line. The rise time of each unit step input is 5 ns. The circuit is simulated using 0.5 mV maximum local truncation error, and the approximation error factor is α =0.1.

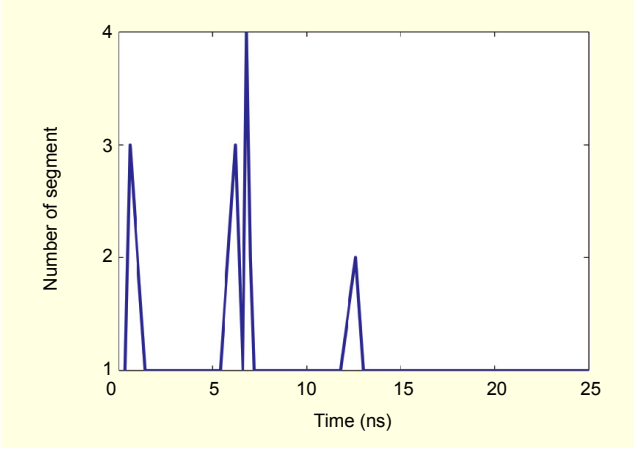

Fig. 11. Variation of number of exponential segments with time of the circuit in Fig. 8.

The simulated waveforms at $v_1(1, t)$ and $v_2(1, t)$ are shown in Figs. 9 and 10 and agree very well with those of Hspice. Figure 11 shows only the number of segments used by our method, indicating fast computation.

In the last example, we demonstrate the advantage of the DSV method that voltage and current distribution can be obtained simultaneously. This event cannot be obtained in a standard circuit simulation such as Hspice without segmenting the line before starting the simulation. This last example circuit, shown in Fig. 12, comprises three transmission lines with a fault within line 1. The line is 1 meter long and has the following distributed parameters:

$$\mathbf{L}=\begin{bmatrix}100 & 25 & 2.5\\ 25 & 100 & 25\\ 2.5 & 25 & 100\end{bmatrix}\text{nH/m},\qquad \mathbf{G}=\begin{bmatrix}1 & 0 & 0\\ 0 & 1 & 0\\ 0 & 0 & 1\end{bmatrix}\text{mS/m},$$

$$\mathbf{C}=\begin{bmatrix}50 & -10 & -1\\ -10 & 60 & -10\\ -1 & -10 & 50\end{bmatrix}\text{pF/m},\qquad \mathbf{R}=\begin{bmatrix}1 & 0 & 0\\ 0 & 1 & 0\\ 0 & 0 & 1\end{bmatrix}\Omega/\text{m}.$$

A fault occurs at x=0.7 m and at 0.4 ps in the form of a 0.4 A current pulse with a 0.2 ps pulse-width, which is about 10 % of the transmission time delay. The distribution voltage across line 2 is shown in Fig. 13.

V. Conclusion

The DSV for time domain simulation of circuit transmission lines has been presented. It transforms the telegraph equation into a state equation that allows the use of conventional techniques to obtain its transient response as well as local truncation error. The PEA method was also introduced to reduce the computational complexity of the DSV method. An algorithm based on a bisection scheme was introduced to segment the line

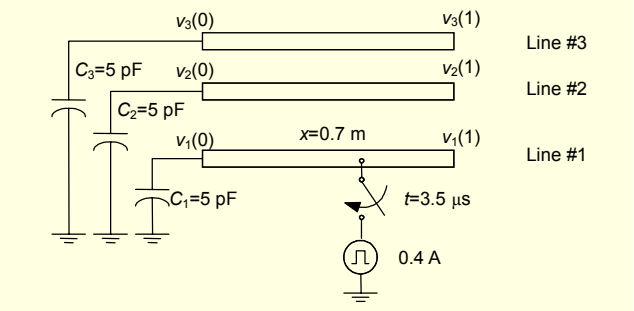

Fig. 12. Circuit comprising 3 lossy transmission lines with fault occurring on one line.

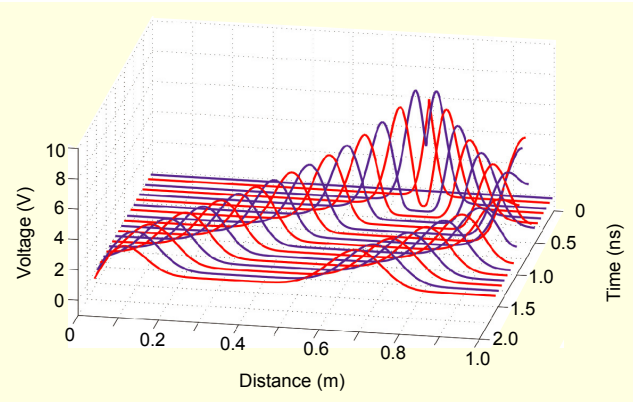

Fig. 13. Line 2 voltage distribution of circuit shown in Fig. 12.

dynamically so that the approximation error is small compared to the local truncation error. Numerical examples showed that this combined DSV-PEA method works very well and requires a small number of segments; therefore, this method can be computationally efficient. However, the calculations of the local truncation error as well as the approximating functions and error require complex matrix calculations such as those shown in the appendix. No CPU time comparison with existing circuit simulations was carried out, and we do not expect our method to execute faster. The key advantages of this method are that its accuracy can be automatically adjusted based on the user specified value of the local truncation error and that the voltage and current distribution can also be obtained without extra calculation or explicit segmentation of a line.

Finally, we give here a short remark about how forward and reflect waves can be computed as by-products of the simulation output.

$$\text{Forward wave: } V^{+}(s)=\frac{1}{2}\left[V_1(s)+Z_c(s)I_1(s)\right] \qquad (22)$$

$$\text{Reflected wave: } V^{-}(s)=\frac{1}{2}\left[V_2(s)+Z_c(s)I_2(s)\right] \qquad (23)$$

Here, $Z_c(s)=\sqrt{(Ls+R)(Cs+G)^{-1}}$.

By performing the inverse Laplace transform, these two equations become

$$v^+(t) = \frac{1}{2}\left[v_1(t) + z_c(t) * i_1(t)\right], \tag{24}$$

$$v^-(t) = \frac{1}{2}\left[v_2(t) + z_c(t) * i_2(t)\right], \tag{25}$$

where $z_c(t) * i_1(t)$ and $z_c(t) * i_2(t)$ are the convolution integrals, which can be time consuming. However, since $Z_c(s)$ is known, it is possible to invert $Z_c(s)$ by using Pade′ approximation [14] which accurately approximates $Z_c(s)$ with a rational function. Partial fraction expansion can be applied to this rational function which can then be inverted. Then, the convolution term can be carried out recursively [15], yielding the required forward and reflected waves at any time point. Note that the time step for recursive convolution can be the same as that used by the DSV method. In that case, the two processes can be carried out in parallel.

Appendix 1.

Lemma 1. This lemma will be needed in A2 and A3.

Let $\mathbf{T}$ and $\mathbf{M}$ be matrices of appropriate dimensions. Then,

$$\int_0^1 e^{\mathbf{M}^T x}\mathbf{T}^T\mathbf{T}e^{\mathbf{M}x}dx = e^{-\mathbf{M}}\begin{bmatrix}0 & \mathbf{I}\end{bmatrix} e^{\begin{bmatrix}-\mathbf{M} & 0\\ \mathbf{T}^T\mathbf{T} & \mathbf{M}^T\end{bmatrix}}\begin{bmatrix}\mathbf{I}\\ 0\end{bmatrix},$$

where $\mathbf{I}$ is an identity matrix of the same dimension as $\mathbf{M}$.

Proof: Let $\mathbf{F}(x) = e^{\begin{bmatrix}-\mathbf{M} & 0\\ \mathbf{T}^T\mathbf{T} & \mathbf{M}\end{bmatrix}x} = \begin{bmatrix}e^{-\mathbf{M}x} & 0\\ \mathbf{Q}(x) & e^{\mathbf{M}x}\end{bmatrix}$.

Then, $\frac{d}{dx}\mathbf{F}(x) = \begin{bmatrix}-\mathbf{M} & 0\\ \mathbf{T}^T\mathbf{T} & \mathbf{M}\end{bmatrix}\begin{bmatrix}e^{-\mathbf{M}x} & 0\\ \mathbf{Q}(x) & e^{\mathbf{M}x}\end{bmatrix}$

$$= \begin{bmatrix}-\mathbf{M}e^{-\mathbf{M}x} & 0\\ \frac{d}{dx}\mathbf{Q}(x) & \mathbf{M}e^{\mathbf{M}x}\end{bmatrix},$$

from which we have

$$\frac{d}{dx}\mathbf{Q}(x) = \mathbf{T}^T\mathbf{T}e^{-\mathbf{M}x} + \mathbf{M}\mathbf{Q}(x) \quad \text{with} \quad \mathbf{Q}(0) = 0.$$

The solution of this differential equation at $x = 1$ is

$$\mathbf{Q}(1) = e^{\mathbf{M}}\int_0^1 e^{-\mathbf{M}x}\mathbf{T}^T\mathbf{T}e^{\mathbf{M}x}dx.$$

Hence, $\int_0^1 e^{-\mathbf{M}x}\mathbf{T}^T\mathbf{T}e^{\mathbf{M}x}dx = e^{-\mathbf{M}}\mathbf{Q}(1)$.

Substitute $\mathbf{Q}(1)$ from the definition of $\mathbf{F}(x)$ to end the proof. □

Appendix 2. Numerical Formula for Computing LTE_n in (13)

From (13) and (15), we have

$$LTE_n = \left\| \mathbf{w}_n(\cdot) - (1 + \frac{h_n}{h_{n-1}})\mathbf{w}_{n-1}(\cdot) + \frac{h_n}{h_{n-1}}\mathbf{w}_{n-2}(\cdot) \right\|.$$

Using the definition in A1, we can rewrite LTE_n as

$$LTE_n = \left\|\mathbf{L}\mathbf{y}(\cdot)\right\| = \left\|\mathbf{L}\, e^{\Gamma x}\mathbf{y}(0)\right\|,$$

where $\mathbf{L} = \begin{bmatrix}\mathbf{0} & \cdots & \mathbf{0} & (\frac{h_n}{h_{n-1}}\mathbf{I}) & (-\mathbf{I} - \frac{h_n}{h_{n-1}}\mathbf{I}) & \mathbf{I}\end{bmatrix}$

Applying the definition of the norm in (12), we obtain

$$LTE_n^2 = \mathbf{y}(0)^T\int_0^1 e^{\Gamma^T x}\mathbf{L}^T\mathbf{T}^T\mathbf{T}\mathbf{L}e^{\Gamma x}dx\,\mathbf{y}(0).$$

Apply the result of lemma 1, and we have

$$LTE_n^2 = \mathbf{y}(0)^T\mathbf{Q}\mathbf{y}(0),$$

where $\mathbf{Q} = e^{-\Gamma}\begin{bmatrix}0 & \mathbf{I}\end{bmatrix} e^{\begin{bmatrix}-\Gamma & 0\\ \mathbf{L}^T\mathbf{T}^T\mathbf{T}\mathbf{L} & \Gamma^T\end{bmatrix}}\begin{bmatrix}\mathbf{I}\\ 0\end{bmatrix}$, and $\mathbf{I}$ is an identity matrix with the same dimension as Γ.

Appendix 3. Numerical Formula for Computing ERR_i

Based on the definitions in (7), let

$$\hat{\mathbf{y}}_n(x) = \begin{bmatrix}\mathbf{y}_n(x)\\ \hat{\mathbf{w}}_n(x)\end{bmatrix},\ \hat{\Gamma} = \begin{bmatrix}\Gamma & 0\\ 0 & \hat{\mathbf{M}}_i\end{bmatrix}, \text{ and } \mathbf{L} = \begin{bmatrix}\mathbf{E_n} & -\mathbf{I}\end{bmatrix}.$$

Then, (7) and (14) can be combined to give

$$\hat{\mathbf{y}}_n(x) = e^{\hat{\Gamma}(x - x_{i-1})}\,\hat{\mathbf{y}}_n(x_{i-1}) \quad \text{for} \quad x_{i-1} \le x \le x_i.$$

Also, ERR_i can be formulated as

$$ERR_i^2 = \int_{x_{i-1}}^{x_i}[\mathbf{L}\hat{\mathbf{y}}_n(x)]^T\ \mathbf{T}^T\mathbf{T}[\mathbf{L}\hat{\mathbf{y}}_n(x)]dx$$

$$= \hat{\mathbf{y}}(x_{i-1})^T\int_{x_{i-1}}^{x_i} e^{\hat{\Gamma}(x - x_{i-1})T}\mathbf{L}^T\mathbf{T}^T\ \mathbf{T}\mathbf{L}e^{\hat{\Gamma}(x - x_{i-1})}dx\ \hat{\mathbf{y}}_n(x_{i-1})$$

$$= (x_i - x_{i-1})\ \hat{\mathbf{y}}(x_{i-1})^T\int_0^1 e^{\hat{\Gamma}\tau T}\mathbf{L}^T\mathbf{T}^T\ \mathbf{T}\mathbf{L}e^{\hat{\Gamma}\tau}d\tau\ \hat{\mathbf{y}}_n(x_{i-1})$$

$$= (x_i - x_{i-1})\ \hat{\mathbf{y}}(x_{i-1})^T\ \mathbf{Q}\ \hat{\mathbf{y}}(x_{i-1}),$$

where $\mathbf{Q} = e^{-\hat{\Gamma}}\begin{bmatrix}0 & \mathbf{I}\end{bmatrix} e^{\begin{bmatrix}-\hat{\Gamma} & 0\\ \mathbf{L}^T\mathbf{T}^T\mathbf{T}\mathbf{L} & \hat{\Gamma}^T\end{bmatrix}}\begin{bmatrix}\mathbf{I}\\ 0\end{bmatrix}$ and $\mathbf{I}$ is an identity matrix with the same dimension as $\hat{\Gamma}$.

References

[1] G. Miano and A. Maffucci, *Transmission Lines and Lumped Circuits*, Academic Press, 2001.

[2] Avant Corporation, *Star-Hspice Manual*, Avant Corporation, CA, 1998.

[3] M. Kizilcay, "Alternative Transients Program Features," 2008 [cited; Available from: http://www.emtp.org/.

[4] National Instruments Corporation, NI Multisim, 2008 [cited July 10, 2008]; Available from: http://www.ni.com/multisim/.

[5] A.C. Antoulas, *Approximation of Large-Scale Dynamical Systems*, SIAM Advances in Design and Control, 2005.

[6] A. Odabasioglu, M. Celik, and L.T. Pileggi, "Prima: Passive Reduced-Order Interconnect Macromodeling Algorithm," *IEEE Trans. Computer-Aided Design of Integrated Circuits and Systems,* vol. 17, no. 8. 1998, pp. 645-654.

[7] D. Saraswat, R. Achar, and M.S. Nakhla, "Passive Reduction Algorithm for Rlc Interconnect Circuits with Embedded State-Space Systems (Press)," *IEEE Trans. Microwave Theory and Techniques*, vol. 52, no. 9. 2004, pp. 2215-2226.

[8] H.W. Dommel, "Digital Computer Solution of Electromagnetic Transients in Single-and Multiphase Networks," *IEEE Trans. Power Apparatus and Systems*, vol. PAS-88, no. 4, 1969, pp. 388-399.

[9] A. Ibrahim et al., "Transmission Line Model for Large Step Size Transient Simulations," *Proc. of the 1999 IEEE Canadian Conf. on Electrical and Computer Engineering*, vol. 2, 1999, pp. 1191-1194.

[10] J. Ogrodzki, *Circuit Simulation Methods and Algorithms*, CRC Press, Inc., 1994.

[11] Z. Tingdong, S.L. Dvorak, and J.L. Prince, "Lossy Transmission Line Simulation Based on Closed-Form Triangle Impulse Responses," *IEEE Trans. Computer-Aided Design of Integrated Circuits and Systems*, vol. 22, no. 6, 2003, pp. 748-755.

[12] J.S. Roychowdhury, A.R. Newton, and D.O. Pederson, "Algorithms for the Transient Simulation of Lossy Interconnect," *IEEE Trans. Computer-Aided Design of Integrated Circuits and Systems*, vol. 13, no. 1, 1994, pp. 96-104.

[13] E. Leelarasmee and P. Naenna, "A Distributed State Variables Approach to the Transmission Lines Transient Simulation," *Proc. the 2004 IEEE Asia-Pacific Conference on Circuits and Systems*, 2004, pp. 73-76.

[14] G.A. Baker and P. G. Morris, *Pade' Approximant Part II: Extensions and Applications*, Addison-Wesley, 1981.

[15] S. Lin and E.S. Kuh, "Transient Simulation of Lossy Interconnects Based on the Recursive Convolution Formulation," *IEEE Trans. Circuit and Systems*, vol. 39, no. 11, 1992, pp. 879-891.

Panuwat Dan-Klang received the BEng degree from Prince of Songkla University, Thailand, in 1998, and the MEng degree from Kasetsart University in 2005. Currently, he is a PhD student at Chulalongkorn University. His research interests include circuit simulation, digital IC design, and wireless sensor networks.

Ekachai Leelarasmee received his BEng degree in EE from Chulalongkorn University, Thailand, in 1974, and his PhD in EE from University of California, Berkeley, USA, in 1982, under the sponsorship of the Anandamahidol Foundation. For his PhD dissertation, in which waveform relaxation was first proposed and applied for time domain analysis of large scale MOS integrated circuits, he received three prestigious awards: the 1983 IEEE Guellemin-Cauer Award, the 1982 IEEE/ACM Design Automation Conference Best Paper Award, and the 1981 U.C. Berkeley D.J. Sakrison Memorial Prize. He is now an associate professor with the Department of Electrical Engineering of Chulalongkorn University. He was the pioneering developer of Thailand's first circuit simulation program LEK, which won two invention awards from the National Research Council of Thailand in 1985 and 1988. His current research interests are circuit simulation programs, closed-caption TV systems, and VLSI designs.